Calculations of hyperfine parameters in tin compounds

A. Svane and N. E. Christensen
Institute of Physics and Astronomy, University of Aarhus, DK-8000 Aarhus C, Denmark

C. O. Rodriguez
IFLYSIB, Grupo de Fisica del Solido, C.C. 565, La Plata 1900, Argentina

M. Methfessel
Institute for Semiconductor Physics, Walter-Korsing-Str. 2, D-15230 Frankfurt(Oder), Germany
(Received 3 December 1996)

With the aim of calibrating Mössbauer spectroscopic measurements, the electric-field gradient and electron contact density is calculated on the Sn nuclear position in a number of Sn compounds representing all kinds of chemical bonding in solids. The full-potential linear-muffin-tin-orbitals method with the local-density approximation for exchange and correlation effects is used. By comparison with experimental ^{119}Sn Mössbauer data the calibration constants relating measured isomer shifts and quadrupole splittings to the electron contact density and the electric-field gradient, respectively, are derived. The difference between the mean square radius of the ^{119}Sn Mössbauer nucleus in its excited isomeric and ground states is found to be $\Delta\langle r^2\rangle = (0.0072 \pm 0.0002)$ fm^2, while the quadrupole moment of the excited ^{119}Sn(24 keV,3/2+) nuclear state is obtained as $|Q| = (12.8 \pm 0.7)$ fm^2. The larger database considered and the use of a more accurate band-structure calculational scheme than in earlier works makes these numbers more accurate and provides improved calibration for Mössbauer spectroscopy. [S0163-1829(97)06917-8]

I. INTRODUCTION

Mössbauer spectroscopy[1,2] is a widely used method for investigations of solid state systems on an atomic scale. Two prominent parameters determined by Mössbauer experiments are the isomer shift, which provides information on the local chemical bond, and the quadrupole splitting, which primarily is a test of the local symmetry around the Mössbauer nucleus. Both quantities depend on the solid state environment as well as on the structure of the nucleus.

The isomer shift of a nuclear transition energy is given by

$$\delta E_{\mathrm{IS}} = \alpha[\rho_a(0) - \rho_s(0)], \tag{1}$$

where $\rho_a(0)$ and $\rho_s(0)$ are the electron charge densities at the nuclear positions (the contact densities) in two different solid state environments, here denoted the absorber (a) and the source (s) materials, respectively. The electron contact densities carry the information on the solid state system, while the calibration constant, α, depends only on the details of the nuclear transition. If δE_{IS} is measured as a relative velocity of the absorber and source materials, α is given by

$$\alpha = \beta \cdot \Delta\langle r^2\rangle, \tag{2}$$

where $\Delta\langle r^2\rangle$ is the difference between the mean square radius of the Mössbauer nucleus in its excited state and its ground state, and β is a numerical constant [for ^{119}Sn, $\beta = 12.7 a_0^3$ mm/(s fm^2), with a_0 being the Bohr radius].[3] If the simplified picture of a uniform sphere is adopted for the nucleus, the calibration constant may be related to the relative change of the nuclear radius as $\alpha = \gamma \Delta R/R$ (with $\gamma = 533 a_0^3$ mm/s for ^{119}Sn).[3]

The quadrupole splitting is caused by the interaction of the nuclear quadrupole moment with the nonspherical part of the crystalline electrostatic potential.[1,4] For an $I = 3/2$ to $I = 1/2$ transition, as in ^{119}Sn, the quadrupole splitting is given by

$$\Delta = \frac{1}{2} e |Q V_{zz}| \left(1 + \frac{1}{3}\eta^2\right)^{1/2}, \tag{3}$$

where e is the elementary charge, Q is the quadrupole moment of the excited state of the Mössbauer nucleus, and V_{zz} and η are the electric-field gradient and asymmetry parameter, respectively, which are determined by the solid state environment. Only the absolute values of Q and V_{zz} enter into Eq. (3).

For the Mössbauer technique to develop into an even more accurate spectroscopy of the solid state, three important aspects have to be addressed. First, the calibration constants, which in essence are the nuclear parameters $\Delta\langle r^2\rangle$ and Q in Eqs. (2) and (3), must be determined to allow a reliable conversion between the measured quantities, i.e., velocities, and the microscopic parameters of the solid, i.e., the electron contact density and the electric field gradient. Second, knowledge must be obtained on how the changes in local chemical environment influence these parameters. The electron contact density and the electric-field gradient are both rather singular quantities, which measure properties of the electron gas at an extreme point, the position of the nucleus, which is far from the region where chemical bonding takes place. Third, reproduction of the measured values by *ab initio* calculations over a wide range of chemical environments shows that the combination of calculations with experiment can be used to gain understanding for systems for which simple intutitive models fail. The present work addresses these points. We will demonstrate that the Mössbauer parameters may be calculated with high precision with the full-

potential linear-muffin-tin-orbitals (FP-LMTO) method[5] within the local-density approximation (LDA) to density functional theory.[6] By a comparison to experimental data we will verify the basic relations (2) and (3) and determine the calibration constants. A wide span of chemical bonding in Sn compounds will be considered. As a result, *ab initio* calculations may now be considered a part of the spectroscopy, in the sense that such calculations may be used as a part of the interpretation of experimental results.[7]

The calibration of Mössbauer experiments has been an issue for a long time.[1,2,8] The nuclear parameters, $\Delta\langle r^2\rangle$ and Q, are, in principle, assessible from first-principles nuclear models, but the accuracy of such models is not always good enough to match the accuracy of Mössbauer experiments. More accurate is the determination of these parameters from comparison of calculated electron contact densities[8] or electric-field gradients[9] with corresponding experimental isomer shifts and quadrupole splittings. The Mössbauer spectroscopy of ^{119}Sn has been theoretically investigated previously.[8,10-12] In Ref. 10 the electron contact density was calculated in a series of tin compounds with the linear-muffin-tin-orbital (LMTO) method[13,14] in the atomic spheres approximation (ASA). In the ASA the crystal volume is divided into atom centered spheres, which are taken slightly overlapping in order to fill a volume equal to the actual crystal volume. Inside the spheres, the potential is taken spherically symmetric, however with a radial form determined by the self-consistent crystalline potential. The ASA introduces some errors into the calculated electron contact density due to the misrepresentation of some parts of space. These errors may usually be ignored for fairly close-packed structures, but in other cases the errors are significant. With the FP-LMTO method all such errors are absent. In the previous study[8,10] of Sn compounds the application of the LMTO method with the ASA to the rutile structured SnO_2 compound was marginally valid, while in the present study a series of open low-symmetry Sn compounds may easily be treated. Additionally, in Refs. 8 and 10 the core electrons of the Sn atom were assumed frozen, while the present work invokes full self-consistent relaxation of the radial shape of the core state wave functions.

The calculation of electric-field gradients using the ASA was considered in Ref. 12, where comparisons with full-potential calculations showed that the ASA correctly describes trends but with reduced quantitative accuracy. Note, however, that the ASA has the advantage of being applicable to disordered systems via the recursion method.[12]

A series of ionic Sn compounds were studied in Ref. 11 by use of the discrete-variational method in the local-density approximation for representative clusters. These authors found that the experimental isomer shifts are well reproduced by their calculations, while the electric-field gradient was less satisfactory, presumably due to the approximations employed for the charge density representation and/or the finite cluster sizes.

In contrast to the previous studies, this paper considers a comprehensive set of Sn compounds, which represent all aspects of chemical bonding and which are treated with a self-consistent full-potential technique. This has two main results. First, a highly reliable calibration of ^{119}Sn Mössbauer experiments is obtained. Second, we can confirm that state-of-the-art *ab initio* LDA calculations consistently lead to good agreement with experiment, at least for the Sn compounds considered here. This underlines the usefulness of combining experiments with such calculations when using Mössbauer spectroscopy to probe a material with an unknown structure.[7]

II. DETAILS OF THE CALCULATIONS

The electronic structures of Sn compounds is calculated with the FP-LMTO method[5] using the LDA for exchange and correlation effects.[6] This method expands the electron wave functions in terms of muffin-tin orbitals,[13] which are atom-centered Neumann functions augmented inside muffin-tin spheres by the numerical solution of the radial scalar-relativistic Dirac equation in the self-consistent crystal potential, together with the energy derivative of this solution.[14] This construction has proven very accurate for solid state calculations.[15] We used three different decay constants for the envelope functions. The basis set included for each atom three orbitals of s character, 3×3 orbitals of p character, and 2×5 orbitals of d character. No shape approximation for the crystal potential is invoked. The crystalline charge density is evaluated exactly within muffin-tin spheres, while in the interstitial region an interpolation scheme is used to obtain the charge density.[5] To increase the accuracy of the interpolation scheme, additional ''empty'' muffin-tin spheres were included for crystal structures with open regions of the unit cell. For the evaluation of the Sn electric-field gradient it was found important to include the Sn $4p$ semicore states as band states, which was done in a separate energy panel. The less deep Sn $4d$ states were included as valence states. Similarly, the O $2s$ and F $2s$ states were included as valence states in the oxides and fluorides.

The electric-field gradient was calculated using the non-spherical part (in fact the $\ell=2$ component) of the crystalline Hartree potential, V_H, from which the second derivative tensor

$$V_{ij}=\frac{\partial V_{H,\ell=2}}{\partial x_i \partial x_j}$$

was obtained. Denoting the eigenvalues of V_{ij} by V_{xx}, V_{yy}, and V_{zz} with $|V_{xx}|\leqslant|V_{yy}|\leqslant|V_{zz}|$, the electric-field gradient per definition is equal to V_{zz}, while the asymmetry parameter is

$$\eta=\frac{V_{xx}-V_{yy}}{V_{zz}},$$

which lies in the range $[0,1]$ (since $V_{xx}+V_{yy}+V_{zz}=0$).

To determine the electron contact density of the Sn nucleus in the Sn compounds, the nucleus was modeled by a uniformly charged sphere of radius $R=1.2A^{1/3}$ fm,[39] where $A=119$ is the mass number of the Sn Mössbauer nucleus. The contact density was obtained as an average over the nuclear volume. All core states were calculated self-consistently in the crystalline environment. In each case considered the experimental structural parameters were used and the number of k vectors in the irreducible wedge of the Brillouin zone was chosen to obtain a well-converged electric-field gradient and electron contact density.

The Sn compounds considered in this work comprise the ionic SnIV compounds, SnF_4, SnO_2, $CaSnO_3$, and $BaSnO_3$, the ionic SnII compounds SnF_2 (α and β), $SnCl_2$, and SnO, together with the compounds of varying ionic-covalent-metallic nature: α-Sn, β-Sn, $SnMg_2$, SnS, Sn_2S_3, SnS_2, SnSe, $SnSe_2$, SnTe, and $SnPd_3$. The electron contact density is determined by the electronic configuration of the Sn atom in the solid state environment. A large effective occupation by $5s$ electrons leads to a large electron contact density, since the $5s$ wave function extends all the way into the nucleus. In contrast, the $5p$ wave function (apart from a small $5p_{1/2}$ component) does not have a finite overlap with the nucleus, but rather effects the electron contact density via an indirect shielding of the $5s$ wave.[16] The SnIV compounds are characterized by a low electron contact density due to the nominal Sn^{4+} configuration of the Sn atom, whereas the SnII compounds have a large electron contact density due to the nominal Sn^{2+} [i.e., (Pd)$5s^2$] configuration. The compounds belonging neither to the SnIV nor to the SnII compounds exhibit electron contact densities of intermediate values.

We now briefly characterize the structures considered in the present calculations.

SnF_4 has a layered body-centered tetragonal structure.[17] Each Sn atom is surrounded by a slightly distorted octahedron of F atoms. The symmetry is D_{4h}^{17} ($I4/mmm$).

SnO_2 has the rutile structure, which is also tetragonal.[17] Each Sn atom is surrounded by a distorted octahedron of O atoms. The symmetry is D_{4h}^{14} ($P4_2/mnm$).

$CaSnO_3$ and $BaSnO_3$ have perovskite structure,[17] i.e., the Sn atoms are located in a simple cubic (O_h^1-$Pm3m$) arrangement with O atoms midway on all cube edges and Ca or Ba in the cube centers. $CaSnO_3$ and $BaSnO_3$ together with SnO_2 are frequently used as reference materials for ^{119}Sn isomer shifts, having essentially identical isomer shifts. Due to its cubic symmetry the Sn atom does not possess an electric-field gradient in the perovskites. In contrast, SnO_2 exhibits a small quadrupole splitting.

SnF_2 is found in three different crystal structures, of which two, the α and β phases, are considered here. The stable form of SnF_2, α-SnF_2, is monoclinic[18] (spacegroup C_{6h}^2-$C2/c$) with eight molecules in the primitive cell. The structure may be viewed as a molecular crystal of Sn_4F_8 tetramers. Two inequivalent Sn atoms are found, one of which is threefold coordinated and the other one fivefold coordinated.[18] β-SnF_2 is orthorhombic (spacegroup D_2^4-$P2_12_12_1$) with four molecules per cell, all equivalent, and with fivefold coordination.[19] The third phase of SnF_2, γ-SnF_2, is a tetragonal structure, but only observed at elevated temperatures. It is reversibly connected with β-SnF_2.[19]

$SnCl_2$ has an orthorhombic structure with four molecules in the unit cell and symmetry D_{2h}^{16} ($Pnam$).[20] All Sn atomic positions are equivalent.

SnO is found in a tetragonal structure with two molecules per unit cell.[17] The two Sn positions are equivalent, and the symmetry is D_{4h}^7 ($P4/nmm$). SnO also exists in a metastable structure (red SnO),[21] the Mössbauer parameters of which have also been determined.[22] Red SnO is orthorhombic, symmetry group C_{2v}^{12} ($C2_1mc$) with four molecules in the unit cell and two inequivalent sites.

The two allotropes of Sn, α-Sn in the diamond structure (O_h^7-$Fd3m$) and β-Sn in the β-Sn structure (D_{4h}^{19}-$I4_1/amd$),[17] are characterized by strong and semistrong covalent bonds, respectively, as is the $SnMg_2$ compound in the fluorite structure (O_h^5-$Fm3m$).

The tin monochalcogenides SnS and SnSe have an orthorhombic structure with four molecules per unit cell, space group D_{2h}^{16} ($Pnam$), which may be regarded as a distorted rocksalt structure. SnTe likewise exists in a slightly distorted rocksalt structure at low temperature. Upon heating, the structure returns to the ideal rocksalt, in SnS and SnSe around 800 K,[23] and in SnTe at 160 K,[24] or below, depending on the carrier concentration.[25] In the present work we only consider SnTe in the ideal rocksalt structure (O_h^5-$Fm3m$).

$SnPd_3$ is found in the cubic $AuCu_3$ structure (O_h^1-$Pm3m$), and SnS_2 and $SnSe_2$ in the hexagonal CdI_2 structure (spacegroup D_{3d}^3-$P\bar{3}m1$). Sn_2S_3 has an orthorhombic structure with four molecules in the unit cell.[26] The symmetry is D_{2h}^{16} ($Pnam$). This compound is peculiar by having two distinct Sn positions (in equal proportions) with different formal valency. The crystal may be viewed as consisting of chains of Sn_2S_3 molecules along the crystalline c axis. The SnIV atom sits in the interior of the chain with six S nearest neighbors in a slightly distorted octahedral coordination. The SnII atom is situated on the side of the chain and bonding to three S atoms. The local chemical environments of the two Sn sites are therefore very similar to those of Sn in SnS_2 and SnS, respectively. Experimentally, the two Sn sites are readily resolved by Mössbauer spectroscopy.[27,28]

III. RESULTS

The calculated electron contact densities and electric-field gradients of Sn compounds are listed in Table I together with experimental information on ^{119}Sn isomer shifts and quadrupole splittings. All isomer shifts are given relative to an oxide source and refer to $T=0$. The experimental accuracy is not quoted, but is typically of the order 0.01–0.05 mm/s. The calculated values are converged to the digits shown, but are of course subject to systematic errors, which are difficult to assess. These include, for example, the validity of the LDA, the scalar relativistic approximation, and other approximations of the calculational scheme, as, e.g., the fitting procedure for the charge density in the interstitial region and the restriction to only one principal quantum number per ℓ channel in the valence bands. One conclusion to be drawn from the present work is that these factors do not cause significant errors.

The degree of agreement between experiment and theory may be judged from plots of the experimental versus theoretical values, which are shown in Figs. 1 and 2. In Fig. 1 the experimental isomer shifts are plotted against the calculated electron contact densities. The straight line through the points in Fig. 1 confirms relationship (1), with the remaining scatter around the line reflecting the combined experimental and theoretical uncertainty. From a best linear fit we derive the calibration constant of Eq. (1):

TABLE I. Calculated electron contact densities, $\rho(0)$, electric-field gradients, V_{zz}, and asymmetry parameters, η, together with experimental isomer shifts, $\delta E_{\rm IS}$, and quadrupole splittings, Δ, for 18 Sn compounds. Units are a_0^{-3} for the electron contact densities, where a large constant ($182\,700 a_0^{-3}$) has been subtracted. The electric-field gradients are in units of 10^{21} V/m^2, and the isomer shifts and quardrupole splittings in units of mm/s.

Compound	$\rho(0)$	$\delta E_{\rm IS}$	V_{zz}	η	Δ
SnF_4	54.16	−0.36 [a]	−19.08	0	1.82 [a]
SnO_2	57.98	0 [b]	−5.87	0.81	0.57 [c]
$CaSnO_3$	54.23	0 [b]	0	0	0
$BaSnO_3$	56.59	0 [b]	0	0	0
α-SnF_2	92.81	3.47 [d]	−19.92	0.28	1.63 [d]
	94.18		−20.41	0.05	
β-SnF_2	93.46	3.12 [d]	−30.44	0.10	2.11 [d]
$SnCl_2$	100.02	4.06 [e]	−6.18	0.89	0.66 [e]
SnO	85.87	2.64 [f]	−16.37	0	1.33 [f]
α-Sn	79.02	2.02 [b]	0	0	0
β-Sn	86.16	2.54 [b]	+4.52	0	0.43 [g]
$SnMg_2$	76.05	1.86 [b]	0	0	0
SnS	94.47	3.29 [h]	+11.05	0.27	0.96 [i]
Sn_2S_3 IV	71.43	1.02 [i]	−4.31	0.45	0.0 [i]
II	95.41	3.34 [i]	−10.55	0.96	0.93 [i]
SnS_2	70.59	0.98 [i]	+0.23	0	0.0 [i]
SnSe	92.08	3.31 [j]	−9.01	0.29	0.81 [j]
$SnSe_2$	73.35	1.36 [k]	−0.05	0	0.0 [k]
SnTe [l]	93.62	3.46 [b]	0	0	0
$SnPd_3$	75.75	1.76 [b]	0	0	0

[a]Reference 29.
[b]Reference 30.
[c]Average value of Refs. 31 and 32.
[d]Reference 33.
[e]Reference 34.
[f]Reference 35.
[g]Reference 31.
[h]Average value of Refs. 24, 31, 28, and 36.
[i]Reference 28.
[j]Average value of Refs. 24 and 37.
[k]References 37 and 38.
[l]Rocksalt structure.

$$\alpha = (0.092 \pm 0.002) a_0^{-3} \ \text{mm/s} \tag{4}$$

or, using Eq. (2),

$$\Delta \langle r^2 \rangle = (0.0072 \pm 0.0002) \ \text{fm}^2. \tag{5}$$

Compared to the previous calibration[10] the present work considers more compounds and a wider span of ^{119}Sn isomer shifts, from SnF_4 with an isomer shift of −0.36 mm/s to $SnCl_2$ with an isomer shift of 4.06 mm/s. In particular, Ref. 10 considered only SnO_2 among the (nominal) Sn^{4+} compounds, and as already stated, a considerable uncertainty is associated with ASA calculations of compounds with the rutile structure. In the present more accurate calculations the electron contact density of Sn in SnO_2 is indeed significantly higher than in Ref. 10, and since the calibration of Ref. 10 is rather sensitive to the value of the SnO_2 electron contact density, this explains why the present calibration constant is ~30% larger. The recent calibration of Ref. 11 found $\alpha = (0.084 \pm 0.007) a_0^{-3}$ mm/s in good agreement with the present, Eq. (4).

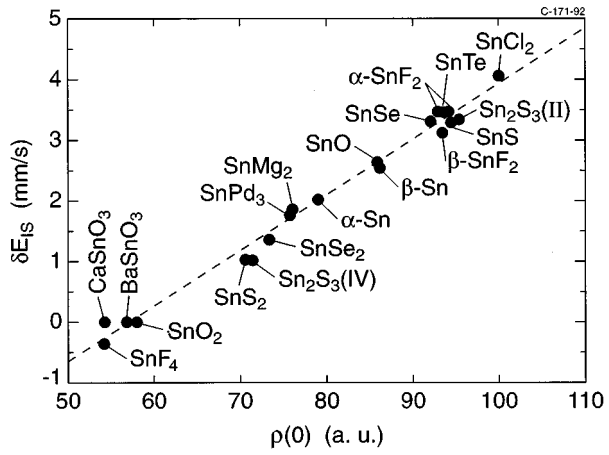

FIG. 1. Calculated electron contact density (in a_0^{-3}) compared to experimental isomer shifts (in mm/s relative to $CaSnO_3$) for tin compounds. A large constant ($182\,700 a_0^{-3}$) is subtracted from the calculated electron contact density.

The total variation in electron contact density in the Sn compounds considered here is ~50 a.u., of which the maximal variation of the core state contribution is 3.6 a.u. (between SnF_4 and SnTe). This means that the relaxation of the core state wave functions to the actual crystalline potential has only a minor effect on the electron contact density in comparison to the variation in $5s$ valence electron contribution.[10] In other cases, like ^{57}Fe and rare earths, the relaxation of core states is much more crucial.[39] It is important to realize that even the nominal Sn^{4+} compounds SnF_4, SnO_2, $BaSnO_3$, and $CaSnO_3$ have a significant $5s$ density at the nucleus. For example, in SnF_4, $\rho_{5s}(0) = 43.8$ a.u., where for comparison, in β-SnF_2, $\rho_{5s}(0) = 83.1$ a.u. The integrated Sn $5s$ charge density in a sphere of radius 2.1 a.u. around the Sn atom reveals 0.49 $5s$ electrons in SnF_4 and 0.90 $5s$ electrons in β-SnF_2. We conclude that the ideal nominal configurations of Sn atoms in solids have only a qualitative significance.[40,8] This is also clear from the large spread in isomer shifts for the class of nominal Sn^{2+} compounds, where the more ionic compounds, SnO and SnF_2,

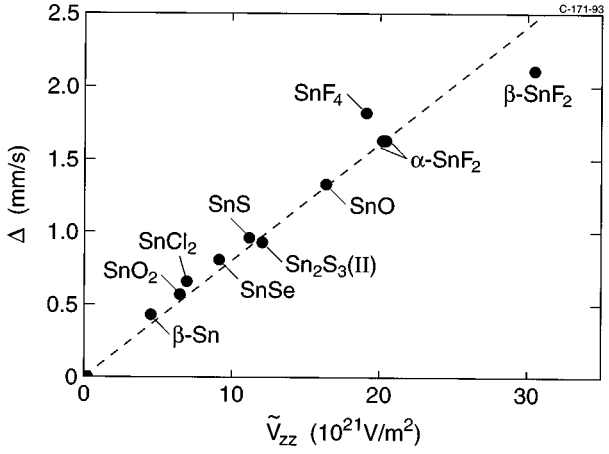

FIG. 2. Calculated electric-field gradient including the asymmetry correction, $\tilde{V}_{zz} = |V_{zz}|(1 + \frac{1}{3}\eta^2)^{1/2}$ (units 10^{21} V/m^2) compared to experimental quadrupole splittings (in mm/s) for tin compounds.

exhibit lower isomer shifts than the less ionic, SnS and $SnCl_2$. The reason for this behavior is that a larger fraction of $5s$ electrons are dragged from the Sn atom in the more ionic compounds, thus leading to a lower electron contact density.

The three widely used ^{119}Sn Mössbauer reference materials $CaSnO_3$, $BaSnO_3$, and SnO_2 are commonly regarded as having identical Sn electronic structure, but the present calculations actually find some variation in the electron contact density between these compounds. In fact, $CaSnO_3$ is that compound for which the deviation from the best straight line in Fig. 1 is largest. It is doubtful, though, if these differences may be detected experimentally.

Figure 2 shows the measured quadrupole splittings plotted against the theoretical electric-field gradients [including the factor $(1+\frac{1}{3}\eta^2)^{1/2}$ for the asymmetry dependence, cf. Eq. (3)]. The fairly good linear relationship confirms relation (3) and we derive a value of

$$|Q| = (12.8 \pm 0.7) \ \text{fm}^2 \tag{6}$$

for the absolute value of the nuclear quadrupole moment of the isomeric ^{119}Sn(24 keV,3/2+) state. This compares favorably with the experimental estimate of $Q = -(10.9 \pm 0.8)$ fm^2.[41] The sign of the nuclear quadrupole moment is not determined by the present work, since Mössbauer spectra do not reveal this quantity directly. The electric-field gradient of β-$SnFe_2$ is calculated somewhat larger than observed experimentally, while that of SnF_4 comes out too small in the calculation.

The two crystallographically inequivalent sites in α-SnF_2 have almost identical electron contact density and electric-field gradient, and presumably the experimental resolution of the two sites is not possible.

For completeness, we briefly discuss the results for some specific compounds in the following. In SnTe we considered only the rocksalt structure, since the crystallographic data on the low-temperature phase are uncertain and apparently dependent on carrier (vacancy) concentration.[25] The transformation to a phase with a lower than cubic symmetry is, however, readily observed in Mössbauer spectroscopy by the appearance of a nonvanishing quadrupole splitting, $\Delta \sim 0.31$ mm/s.[24]

We have also considered the red form of SnO, which was reported to have a large quadrupole splitting (2.20 mm/s in Ref. 22, 1.99 mm/s in Ref. 31) and an isomer shift of 0.60 mm/s relative to α-Sn (0.11 mm/s lower than black SnO). We find, however, that the two crystallographic Sn sites of red SnO have widely different electric-field gradients, so that an interpretation in terms of a single quadrupole doublet is not appropriate. One Sn site, Sn_1 with coordinates (0,0,0) in the orthorhombic unit cell,[21] has a field gradient of -16.10×10^{21} V/m^2, while the other site, Sn_2 with coordinates (0, 0.441, 0.254) in the cell, has a field gradient of -31.69×10^{21} V/m^2, i.e., almost twice as large. The electron contact density differs slightly, being 88.42 a.u. and 84.06 a.u. for the Sn_1 and Sn_2 positions, respectively. Therefore, we encourage that the Mössbauer spectrum of red SnO be analyzed in terms of two quadrupole split lines.

For Sn_2S_3 we find distinct hyperfine parameters for the two inequivalent Sn positions, as is also observed experimentally. The electron contact densities of the SnII and SnIV atoms are close to those found in SnS and SnS_2, respectively, as anticipated from the similar local chemical environments. Both sites exhibit a nonzero electric-field gradient. At the SnIV site the field gradient is -4.31×10^{21} V/m^2, which would correspond to an experimental quadrupole splitting of 0.33 mm/s, which is barely observable, and thus in agreement with experiments, which do not report any quadrupole splitting for this site.[27,28] The electric-field gradient at the SnII site is -10.55×10^{21} V/m^2, i.e., much larger in magnitude, and also the asymmetry parameter, $\eta = 0.96$, is very large. This corresponds to a quadrupole splitting of 0.90 mm/s, which is in excellent agreement with the experimentally observed splitting of 0.90 mm/s,[27] or 0.93 mm/s.[28] The agreement with the value for the field gradient calculated (and measured) in SnS must be considered accidental, since the asymmetry is rather different.

To test the accuracy of the present calculational scheme for obtaining the electric-field gradient in solids we have, for the case of rutile SnO_2, performed a full-potential linear-augmented-plane-wave[42] (FP-LAPW) calculation for this compound. With the FP-LAPW method, the Sn and O electric-field gradients are calculated to be -5.66×10^{21} V/m^2 and -9.81×10^{21} V/m^2 with asymmetry parameters $\eta = 0.92$ and $\eta = 0.06$, respectively. With the full-potential LMTO method we find the field gradients to be -5.87×10^{21} V/m^2 and -10.94×10^{21} V/m^2 with asymmetry parameters $\eta = 0.81$ and $\eta = 0.10$ for Sn and O, respectively. Since both the applied methods may be considered highly accurate for electronic structure calculations of solids, these numbers demonstrate the level of accuracy (i.e., $\sim 10\%$) one can expect for a somewhat singular quantity like the electric-field gradient.

IV. CONCLUSIONS

Electronic structure calculations for a series of Sn compounds comprising all aspects of chemical bonding were presented. The electron contact density and electric-field gradient of Sn nuclei were calculated and compared to experimental isomer shifts and quadrupole splittings with good linear relationships. As a consequence accurate values for the difference in mean square radius of the nuclear states, $\Delta\langle r^2\rangle = (0.0072 \pm 0.0002)$ fm^2, and ^{119}Sn(24 keV,3/2+) excited state quadrupole moment, $|Q| = (12.8 \pm 0.7)$ fm^2 were obtained. In addition to this accurate calibration of ^{119}Sn Mössbauer spectroscopy the present work confirms that state-of-the-art electronic structure calculational schemes based on the local-density approximation can be used to compute hyperfine parameters in agreement with experiments. This introduces the new aspect for the future of combining experiments and calculations for investigations of systems of unknown structure.

ACKNOWLEDGMENTS

This work was supported by the Danish Natural Science Research Council, Grant No. 11-0694 and by the Commission of the European Communities, Contract No. CI1-CT92-0086.

[1] N. N. Greenwood and T. C. Gibb, *Mössbauer Spectroscopy* (Chapman and Hall, London, 1971).
[2] *Mössbauer Isomer Shifts*, edited by G. K. Shenoy and F. E. Wagner (North-Holland, Amsterdam, 1978).
[3] G. K. Shenoy and B. D. Dunlap, *Mössbauer Isometer Shifts* (Ref. 2), App. IV.
[4] M. H. Cohen and F. Reif, Solid State Phys. **5**, 321 (1957).
[5] M. Methfessel, Phys. Rev. B **38**, 1537 (1988); M. Methfessel, C. O. Rodriguez, and O. K. Andersen, *ibid.* **40**, 2009 (1989).
[6] R. O. Jones and O. Gunnarsson, Rev. Mod. Phys. **61**, 689 (1989). We use the parametrization of S. H. Vosko, L. Wilk, and M. Nusair, Can. J. Phys. **58**, 1200 (1980).
[7] M. Fanciulli, C. Rosenblad, G. Weyer, A. Svane, N. E. Christensen, and H. von Känel, Phys. Rev. Lett. **75**, 1642 (1995); M. Fanciulli, A. Zenkevich, I. Wenneker, A. Svane, N. E. Christensen, and G. Weyer, Phys. Rev. B **54**, 15 985 (1996).
[8] A. Svane and E. Antoncik, Phys. Rev. B **34**, 1944 (1986).
[9] P. Dufek, P. Blaha, and K. Schwarz, Phys. Rev. Lett. **75**, 3545 (1995).
[10] A. Svane and E. Antoncik, Phys. Rev. B **35**, 4611 (1987).
[11] J. Terra and D. Guenzberger, Phys. Rev. B **44**, 8584 (1991); Hyperfine Interact **60**, 627 (1990); J. Phys. Condens. Matter **3**, 6763 (1991).
[12] H. M. Petrelli and S. Frota-Pessoa, J. Phys. Condens. Matter **2**, 135 (1990); M. Methfessel and S. Frota-Pessoa, *ibid.* **2**, 149 (1990).
[13] O. K. Andersen, Phys. Rev. B **12**, 3060 (1975).
[14] H. L. Skriver, *The LMTO Method* (Springer-Verlag, Berlin, 1984).
[15] O. K. Andersen, O. Jepsen, and O. Glötzel, in *Canonical Description of the Band Structures of Metals*, Proceedings of the International School of Physics, Course LXXXIX, Varenna, 1985, edited by F. Bassani, F. Fumi, and M. P. Tosi (North-Holland, Amsterdam, 1985), p. 59.
[16] A. Svane, Phys. Rev. Lett. **60**, 2693 (1988).
[17] R. W. G. Wyckoff, *Crystal Structures* (Wiley, New York, 1964), Vols. 1 and 2.
[18] G. Denes, J. Pannetier, J. Lucas, and J. Y. Le Marouille, J. Solid State Chem. **30**, 335 (1979).
[19] G. Denes, J. Pannetier, and J. Lucas, J. Solid State Chem. **33**, 1 (1980).
[20] J. M. van den Berg, Acta Crystallogr. **14**, 1002 (1961).
[21] J. D. Donaldson, W. Moser, and W. B. Simpson, Acta Crystallogr. **16**, A22 (1963).
[22] C. G. Davies and J. D. Donaldson, J. Chem. Soc. A **1968**, 946.
[23] T. Chattopadhyay, J. Pannetier, and H. G. von Schnering, J. Phys. Chem. Solids **47**, 879 (1986).
[24] V. Fano and I. Ortalli, J. Chem. Phys. **61**, 5017 (1974).
[25] L. J. Brillson, E. Burstein, and L. Muldawer, Phys. Rev. B **9**, 1547 (1974).
[26] D. Mootz and H. Puhl, Acta Crystallogr. **23**, 471 (1967); R. Kniep, D. Mootz, U. Severin, and H. Wunderlich, Acta Crystallogr. B **38**, 2022 (1982).
[27] G. Amthauer, J. Fenner, S. Hafner, W. B. Holzapfel, and R. Keller, J. Chem. Phys. **70**, 4837 (1979).
[28] J. Grothaus and P. Boolchand, J. Non-Cryst. Solids **72**, 1 (1985).
[29] L. Fournès, J. Grannec, Y. Potin, and P. Hagenmuller, Solid State Commun. **59**, 833 (1986).
[30] J. G. Stevens, Hyperfine Interact. **13**, 221 (1983).
[31] J. K. Lees and P. A. Flinn, J. Chem. Phys. **48**, 882 (1968).
[32] H. A. Stöckler, H. Sano, and R. H. Herber, J. Chem. Phys. **45**, 1182 (1966).
[33] T. Birchall, G. Denes, K. Ruebenbauer, and J. Pannetier, J. Chem. Soc. (London) Dalton Trans. **1981**, 1831 (1981).
[34] S. R. A. Bird, J. D. Donaldson, and J. Silver, J. Chem. Soc. (London) Dalton Trans., **1972, 1950 (1972).**
[35] R. H. Herber, Phys. Rev. B **27**, 4013 (1983).
[36] J.-C. Jumas, S. del Bucchia, E. Phillippot, and M. Maurin, J. Solid State Chem. **41**, 50 (1982).
[37] P. Boolchand, J. Grothaus, W. J. Bresser, and P. Suranyi, Phys. Rev. B **25**, 2975 (1982).
[38] R. H. Herber, A. E. Smelkinson, M. J. Sienko, and L. F. Schneemeyer, J. Chem. Phys. **68**, 3705 (1978).
[39] A. J. Freeman and D. E. Ellis, *Mössbauer Isomer Shifts* (Ref. 2), Chap. 4.
[40] E. Antoncik, Phys. Rev. B **23**, 6524 (1981).
[41] H. Haas, M. Menningen, H. Andreasen, S. Damgaard, H. Grann, F. T. Pedersen, J. W. Petersen, and G. Weyer, Hyperfine Interact. **15/16**, 215 (1983).
[42] P. Blaha, K. Schwarz, P. Dufek, and R. Augustyn, WIEN95, Technical University of Vienna 1995 [improved and updated Unix version of the original copyrighted WIEN code, which was published by P. Blaha, K. Schwarz, P. Sorantin, and S. B. Trickey, in Comput. Phys. Commun. **59**, 399 (1990)]; P. Blaha, K. Schwarz, and P. H. Dederichs, Phys. Rev. B **37**, 2792 (1988).